Self-induced attenuation of pulsed laser radiation in an aqueous suspension of submicron light-absorbing particles

2003 J. Phys.: Condens. Matter 15 6647

(http://iopscience.iop.org/0953-8984/15/40/003)

INSTITUTE OF PHYSICS PUBLISHING JOURNAL OF PHYSICS: CONDENSED MATTER

J. Phys.: Condens. Matter **15** (2003) 6647–6657 PII: S0953-8984(03)58425-9

Self-induced attenuation of pulsed laser radiation in an aqueous suspension of submicron light-absorbing particles

S E Zelensky

Physics Department, Kyiv University, 6 Glushkova street, Kyiv 03680, Ukraine

E-mail: zele@phys.univ.kiev.ua

Received 8 January 2003, in final form 28 July 2003
Published 26 September 2003
Online at stacks.iop.org/JPhysCM/15/6647

Abstract

In this paper, the interaction of Q-switched YAG:Nd^{3+} laser radiation of moderate intensity (up to 50–100 MW cm^{-2}) with an aqueous suspension of submicron light-absorbing particles is investigated. The experiments reveal significant self-induced attenuation of laser radiation which is accompanied by laser-induced incandescence of suspended particles. The transformation of shape is also observed for the laser pulses propagating through the suspension and for the scattered pulses. A model is proposed which describes the experimental data obtained. The model supposes that gaseous shells grow around the laser-heated particles due to the vaporization of surrounding water. With the use of the proposed model, calculations were performed for the optical transmittance of the cell and for the shape of the transmitted and scattered laser pulses. The calculated and experimental data are in satisfactory agreement with each other. It is also concluded that only a small fraction (approximately 0.01–0.5%) of the laser-heated particle energy is spent in evaporation of the surrounding water.

1. Introduction

As is known, radiation of a high-power pulsed laser in the range of laser power densities below the plasma formation threshold can cause significant overheating of microscopic light-absorbing particles. For example, laser-induced heating of soot particles suspended in gases (in flames, in engine exhausts) is investigated in [1–7]. As is shown for soot particles and aggregates ranging approximately from 1 nm to 10 μm in size, a Q-switched laser pulse can increase the particle temperature up to the vaporization temperature of carbon, approximately 4000 K. At such conditions, particle thermal emission (laser-induced incandescence, LII) is experimentally observed. As the local temperature reaches thousands of kelvin, the emission spectra of LII become wide (from ultraviolet to infrared) and smooth. The LII spectra can be fitted by Planck's black-body emission formula, but such an approximation is rough, because

the particles are not uniform in size, the laser power is spatially non-uniform, etc. The laser power dependence of the LII signal is essentially non-linear. Excitation curves of LII usually include a rapid increase, a plateau and a gradual decrease of LII signal with laser power. LII is now a rapidly developing diagnostic method for aerosols.

LII is also observed in condensed matter, when light-absorbing microscopic particles are suspended in a transparent matrix. For example, microscopic inclusions in some oxide glasses and submicron pigment particles in water can be heated to incandescent temperatures by a Q-switched laser [8–10]. Turbid natural water also emits white light under powerful laser excitation. LII in condensed matter has been far less investigated than LII in the gaseous phase. In both cases, LII has some similar phenomenological properties (wide emission spectrum, non-linear response to laser excitation); however, certain differences are worth noting. There is no plateau in the excitation curve of LII in condensed matter and the duration of LII signals is shorter.

Concerning the interactions of light-absorbing microscopic particles with powerful pulsed laser radiation, we should also mention the complicated effects of laser-induced transformations of micron-sized droplets irradiated by powerful lasers [11–19]. Experiments have been performed with various droplets (water, ethanol, diesel, CCl_4, bromoform, water with light-absorbing dyes, etc) and lasers (carbon dioxide, YAG:Nd^{3+}). For example, wavelengths of CO_2 lasers are suitable for heating water droplets. The experiments have shown the laser-induced explosive vaporization of droplets. Depending on the spatial distribution of laser power within the droplet (uniform or non-uniform), the laser-induced vapour cloud can be symmetric about the droplet centre, or asymmetric, with plumes of vapour and/or hot liquid from the shadow and/or illuminated faces of the droplet. Theoretical interpretation of the phenomena observed is based on the droplet superheating.

Laser-induced explosion of water droplets is a physical mechanism of the phenomenon of self-enhanced transparency [19] which is observed in the interaction of a CO_2 laser radiation with water aerosol particles. Experiments have shown that powerful pulsed laser radiation vaporizes the droplets and hence a significant enhancement of transmission is observed together with transformation of the shape of the transmitted laser pulse.

The above-mentioned phenomena caused by laser-induced heating of micron-sized objects are observed at moderate intensities of laser radiation—from 10 to 100 MW cm^{-2}. It is easy to estimate that such levels of laser power density are sufficient for heating a microscopic object to a temperature of thousands of kelvin. Nevertheless, in the experiments with laser-heated droplets, no signs of thermal emission were observed. This circumstance is possibly an indication of the unique properties of energy dissipation in laser–droplet interactions.

The following feature of LII seems to be noteworthy. LII in glass is observed at laser surface power densities of the order of 50–100 MW cm^{-2}, whereas in aqueous suspensions and in gases it can be reliably detected at much smaller laser intensities (7–10 MW cm^{-2}). Such differences can be related to the differences in the mechanisms of energy dissipation of laser-heated particles.

In order to clarify the mechanism of interaction of submicron suspended particles in aqueous suspensions with pulsed laser radiation, in this paper the phenomena are investigated which accompany LII in an aqueous suspension at moderate levels of laser excitation, up to 50–100 MW cm^{-2}.

2. Experimental details

In the present work, a computer-assisted spectrometer was employed with a Q-switched YAG:Nd^{3+} laser (wavelength $\lambda = 1.06$ μm, pulse duration $\tau_i = 25$ ns FWHM). The

transmittance of a cell with the suspension under investigation was measured as a ratio of the energies of the laser pulses: namely, the transmitted pulse energy over the incident pulse energy. The pulse energies were measured with phototubes together with integrating circuits. The laser operated in a single-pulse regime so that each of the pulses from the phototubes was integrated and digitized separately. The LII optical signals were detected by a photomultiplier through a single grating monochromator. To eliminate scattered laser light, the LII measurements were performed with a cutoff glass filter installed inside the monochromator. Further, the photomultiplier was blind at the laser wavelength. The oscillograms of the laser pulses were recorded with a phototube with a response time of 0.5 ns and with a strobe oscillograph.

As the suspension of black-body particles we used a suspension of black gouache paint in distilled water. Every paint is a mixture of microscopic pigment particles in a transparent liquid vehicle. Unlike soluble dyes, pigments are chemicals that do not dissolve in water or the vehicle. For these experiments, the paint was diluted in water (approximately 1:1000) so that its optical transmittance becomes sufficient for observation of the phenomena under investigation. The number density of pigment particles in the prepared suspension is unknown. However, the model proposed in this paper does not require knowledge of the particle concentration.

Unlike the experiments [9] where the suspension investigated was well diluted and therefore the non-depleted field approximation was valid for the laser radiation, in the present experiments the paint concentration is increased so that significant attenuation of laser radiation takes place due to the absorption and scattering by the suspended particles in the cell. For a cell thickness of $d = 2$ cm the low-signal transmittance at the laser wavelength was $T_0 = 0.73$.

For the black paint used in this work, the chemical composition of the black pigment was unknown. Typical black pigments can be soot, manganese dioxide and ferrite, copper chromite spinel, etc. However, chemical composition seems to be a secondary factor for the capability of observation of LII. For example, LII is clearly observable with violet paint (possibly made of cobalt oxide pigments), and, even more, LII can be observed in turbid natural water. Thus, for various particles, the laser fluences necessary for the observation of LII can be different.

Particles in a paint are not uniform in size and shape. Typically, particles in paints are 0.01–5 μm in size. Different manufacturers have different standards for pigment size. In this paper, microscopic observation did not reveal particles with a size exceeding 1 μm. Measurements performed with a nephelometer show an average particle radius of approximately 0.1 μm. Since the investigated suspension consists of particles of various sizes, the calculations in this paper were performed for two values of particle radius, one of them well below the wavelength and the other of the order of magnitude of the wavelength. In both cases, the results of the calculations were qualitatively similar.

All of the experiments were performed at room temperature. To eliminate errors caused by the laser-induced fading, the investigated suspension was pumped through the cell at a flow rate of 0.5 l min^{-1}; thus each of the laser pulses interacted with a 'fresh' portion of the suspension.

3. Results and discussion

Figure 1 shows the optical transmittance, T, of a cell as a function of the incident laser surface power density, F_0. As can be seen from figure 2, the cell transmittance becomes substantially smaller with an increase of laser power density, i.e. the self-induced attenuation of laser radiation takes place. The experiments also show that LII becomes detectable in the suspension in the range of $F_0 = 6$–8 MW cm^{-2} where the decrease of the cell transmittance is observed. The presence of LII indicates the laser heating to be the primary mechanism for the interaction of the suspended particles with laser radiation.

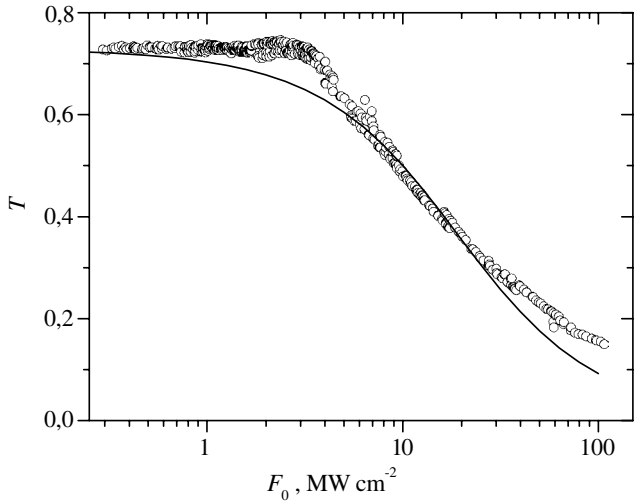

Figure 1. Cell transmittance, T, as a function of incident laser surface power density, F_0. Circles: experiment; solid curve: calculation.

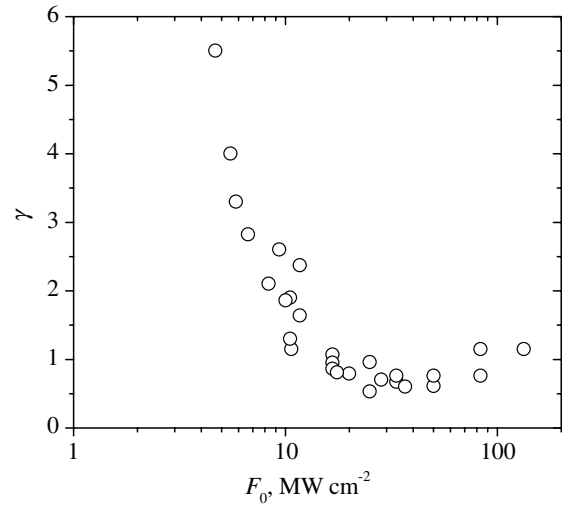

Figure 2. The parameter γ measured at an LII wavelength of 500 nm as a function of F_0.

As is shown in previous works [8, 9], a convenient characteristic of LII is the parameter $\gamma = \Delta(\lg P_{\mathrm{LII}})/\Delta(\lg F)$, where P_{LII} is the power of the LII optical signal detected at a fixed wavelength, and F is the laser surface power density. In the experiments described in the present work, LII photons were collected from the volume near the entrance window of the cell, and hence F_0 can be substituted instead of F for the calculation of γ. Figure 2 presents the experimentally measured γ at a wavelength of 500 nm as a function of F_0. Note in the figure that γ decreases drastically with an increase of F_0 in the range where LII becomes detectable. Further, at $F_0 > 20$ MW cm^{-2} γ becomes less than or equal to unity.

In [9], where LII in an aqueous suspension of black-body particles was studied in the case of low laser intensities, $F_0 \approx 7$ MW cm^{-2}, the interaction of suspended particles with laser radiation was described with the use of a model which considers the heat transfer to

the environment to be the main mechanism of particle energy dissipation. The model in [9] cannot interpret the data shown in figures 1 and 2 here. It is plausible to suggest that with the increase of laser surface power density a new mechanism of particle energy dissipation begins to operate, and it includes the vaporization of water around the laser-heated particles.

To explain the experimental results obtained, the following model can be used in a first approximation. Consider a spherical black-body particle with a radius r_0 heated by pulsed laser radiation. During the action of the laser pulse, the absorbed laser energy is partially transferred to the surrounding water and causes its vaporization. Hereinafter this process will be considered as the growth of a gaseous shell around a laser-heated particle. Thus the laser-heated particle can be treated approximately as a core–shell spherical particle. The radius of the core is r_0 (neglecting its changes due to the vaporization of the particle's material) and the thickness of the shell is denoted as Δr. The light scattered by the core–shell particles is responsible for the observed self-induced attenuation of the laser radiation (figure 1). The model presumes an approximation that the attenuation of laser light by a suspension of core–shell particles is mainly governed by the particle radius $r = r_0 + \Delta r$, and does not depend on the internal structure of the particle.

Now consider several simple estimations. In the experiments, the number density, N, of suspended particles is a constant. However, as seen from figure 1, the transmittance of the cell decreases from the value of $T_0 = 0.73$ at $F_0 = 1$ MW cm^{-2} to the value of $T_1 = 0.15$ at $F_0 = 100$ MW cm^{-2}. With the assumption of validity of Bouguer's law, the light attenuation can be characterized by the effective extinction cross-section and the following relations can be written: $\ln T_0 = \sigma_0 N d$, $\ln T_1 = \sigma_1 N d$. Thereby we can evaluate $\sigma_1/\sigma_0 \approx 6$. The effective extinction cross-sections σ_0 and σ_1 are averaged over time (within the laser pulse), over z (within the cell thickness) and over the radii of suspended particles. Here z is the coordinate along the laser beam axis.

According to the proposed model, a core–shell particle can be characterized by an extinction cross-section, $\sigma(t)$, which increases from σ_0 to $\sigma(\tau_i)$ during the laser pulse due to the increase of the shell thickness. For evaluation purposes, the increase of $\sigma(t)$ can be approximated by a linear function of time. Then the effective extinction cross-section σ_1 can be written as $\sigma_1 = [\sigma_0 + \sigma(\tau_i)]/2$ and the ratio of extinction sections at the end of the laser pulse can be estimated as $\sigma(\tau_i)/\sigma_0 = 2\sigma_1/\sigma_0 - 1 \approx 11$. It should be noted that this is still a z-averaged value.

To obtain an estimate of $\sigma(\tau_i)/\sigma_0$ for a given value of $F_0 = 100$ MW cm^{-2}, suppose the extinction cross-section of core–shell particles depends on z similar to the dependence of $F(z)$, i.e. it decreases exponentially. Then, to obtain the ratio of extinction cross-sections $\sigma(\tau_i)/\sigma_0$ at $z = 0$, the above averaged ratio of sections should be multiplied by a factor of $-(1-T_1)^{-1} \ln T_1$. Finally we get the estimate $\sigma(\tau_i)/\sigma_0 \approx 25$ at $z = 0$ and $F_0 = 100$ MW cm^{-2}.

As is known [20], the extinction cross-section of a small spherical particle depends on the particle radius as follows. For small particles with a radius much smaller than the wavelength of the light (Rayleigh regime), the section is proportional to the sixth power of the radius. For large particles with a radius exceeding the wavelength, the section is proportional to the radius squared. For intermediate particles with a radius of the order of the wavelength, the sixth-power function gradually transforms into a quadratic function with slight oscillations. Accordingly, using the above estimate of cross-sections, the ratio of particle radii at $z = 0$, $t = \tau_i$ and $F_0 = 100$ MW cm^{-2}, can be evaluated as $r/r_0 \approx 1.7$ for $r, r_0 < \lambda$ and $r/r_0 \approx 5$ for $r, r_0 > \lambda$.

With these values of r and r_0, the speed of growth of the particle shell can be evaluated as $\Delta r/\tau_i \approx 2.8$ m s^{-1} for $r_0 = 0.1$ μm and $\Delta r/\tau_i \approx 14$–$80$ m s^{-1} for $r_0 = 0.5$ μm. The values of growth rate obtained are of the same order of magnitude as the values of laser-induced

bubble growth rate at a solid–liquid interface [21]. In [21] it is supposed that bubble growth is largely dominated by inertia-controlled processes and the following expression is used:

$$\frac{\mathrm{d}r}{\mathrm{d}t} = \left(\frac{\pi}{7}\frac{p - p_\infty}{\rho_\mathrm{l}}\right)^{1/2}$$

where ρ_l is the density of water and p_∞ is the ambient pressure. With the use of this expression, the internal gas pressure in the particle shell can be estimated as $p = p_\infty + 7\pi^{-1}\rho_\mathrm{l} r^2 \tau_\mathrm{i}^{-2} \approx 1.2 \times 10^5$ Pa for $r_0 = 0.1$ μm and (5.5–140) $\times 10^5$ Pa for $r_0 = 0.5$ μm.

Note that, on the one hand, the investigated laser-induced processes of formation and growth of gaseous shells are relatively quick compared with the laser pulse duration (25 ns) due to the actual existence of the self-induced attenuation of laser pulses. The appropriate rate of particle heating can be estimated as (2–4) $\times 10^{11}$ K s^{-1}. On the other hand, these processes can be considered as relatively slow compared with the acoustic relaxation time. The time necessary for an acoustic relief wave to disperse from the heated zone several microns in size is one-tenth as large as the laser pulse duration—hence 'explosive vaporization' processes [22] seem to be unlikely in the present work.

Now consider several simplified equations which describe the investigated processes to a first approximation. The amount of heat which the laser-heated particle expends in vaporizing the surrounding water during the time interval $\mathrm{d}t$ can be described as follows:

$$GF\sigma_0\,\mathrm{d}t = \Lambda\,\mathrm{d}m \tag{1}$$

where G is the fraction of absorbed laser energy which is spent in vaporizing the water, Λ is the latent heat of vaporization of water, and $\mathrm{d}m$ is the mass of vaporized water. By integrating (1) and with the use of the equation of state for an ideal gas, an approximate expression can be written for the volume of the gaseous shell:

$$V(t) = \frac{R\theta\sigma_0 G}{\mu p \Lambda}\int_0^t F(t')\,\mathrm{d}t' \tag{2}$$

where θ and p are the average gas temperature and pressure respectively, μ is the molar mass of water, and R is the gas constant. With the use of simple geometrical considerations and expression (2), the dependence of the particle radius on time, $r(t)$, can be easily derived for the time interval within the duration of the laser pulse.

Hereinafter the extinction cross-section of a core–shell particle is approximated as follows:

$$\sigma(t) = \begin{cases} \xi[r(t)]^6 & \text{for } r \leqslant \lambda \\ \xi\lambda^4[r(t)]^2 & \text{for } r > \lambda \end{cases} \tag{3}$$

where ξ is the fitting parameter.

Further suppose that the laser radiation propagating through the suspension behaves according to

$$\mathrm{d}F/F = -\sigma N\,\mathrm{d}z. \tag{4}$$

On the basis of expressions (1)–(4), a computer program was written to model the propagation of laser pulses through the suspension. The program includes a cycle of integration over z according to expression (4) and a nested cycle of integration over t according to (2). The time dependence of the laser surface power density is approximated by a Gaussian function as follows:

$$F = F_0 \exp[-(t - t_0)^2 \tau_\mathrm{i}^{-2} 4 \ln 2] \tag{5}$$

where t_0 is the laser pulse peak time. The program calculates the dependence of the cell transmittance on the laser surface power density, and also enables simulation of the transformation of shape of the laser pulse propagating through the suspension.

For the calculations, the numerical values of the parameters were determined as follows. First, for the particle radius in this paper the values of 0.1 and 0.5 μm were used. With the known dependence $\sigma(r)$ from [20], the parameter ξ in (3) is determined and hence σ_0 is calculated for a given r_0. Then the parameter G is temporarily set to zero and the particle number density N is determined by running the program and fitting the calculated transmittance according to the initial condition $T_0 = 0.73$ obtained by experiment (figure 1) at $F_0 < 3$ MW cm^{-2}. The above estimate of gas pressure p is substituted into (2). The calculations were performed over a wide interval of gas temperature, $\theta = 3000$–$10\,000$ K, which corresponds to the estimates of particle temperature [9]. Finally, to calculate the cell transmittance as a function of laser surface power density a single fitting parameter is required—the coefficient G in expression (1). The calculated dependence $T(F_0)$ is shown in figure 1 as a solid curve. As can be seen, the model provides satisfactory agreement between the experimental and calculated data. The disagreement of the calculated function compared with the experimental data at laser intensities of 1–5 MW cm^{-2} can be accounted for by the non-uniform distribution of laser surface power density across the beam.

Within the above limits of gas pressure and temperature in the particle shell, satisfactory agreement between theory and experiment can be obtained for G within the range 8.7×10^{-5}–4.7×10^{-3}. Such small values of G indicate that only a small fraction of the particle energy is spent in evaporating the surrounding water. Nevertheless, it should be noted that the laser-induced growth of gaseous shells around the suspended particles is the main mechanism of self-induced attenuation of the laser beam in the suspension.

As mentioned already, in the literature there are no reports on LII in laser-heated droplets. A plausible explanation might be the following. When a superheated limit temperature (approximately 578 K for water) is reached in the laser-heated droplet, a new powerful mechanism for the dissipation of laser-delivered energy comes into play—namely, the explosive vaporization of the droplet. This mechanism consumes energy and prevents further heating, so LII is not detected. (Incidentally, similar behaviour is observed in the case of LII of soot particles in flames. When a 4000 K threshold is reached, the laser-heated soot begins to evaporate, and the particle temperature becomes a weak function of laser power [7].) However, in the present paper the small values of G indicate a low efficiency of evaporation of the water, and hence the absorbed laser power is sufficient for heating the particles to incandescent temperatures.

When the particle shell increases during the laser pulse, one can expect temporal transformations of shape of a laser pulse propagating through the suspension. Numerical simulations show that the following transformations of a laser pulse can be expected with an increase of laser surface power: (i) the pulse area decreases according to figure 1; (ii) the pulse width decreases; and (iii) the pulse peak shifts towards the front edge. The calculations of $F(z, t)$ were performed within the above-mentioned limits of the parameters p, θ, r_0 and G. If these parameters are fitted for the best agreement of the cell transmittance data (figure 1), the calculations show that the shape of the laser pulse transmitted through the suspension is determined by the value of the incident laser power density F_0. Figure 3(a) shows the calculated oscillograms (i.e. F/F_0 as a function of t), where the numbers near the curves are values of F_0 in MW cm^{-2}.

The experiments confirm the predicted transformation of shape of a laser pulse propagating through the suspension. Figure 4(a) shows the experimental oscillograms of laser pulses transmitted through the cell, where the numbers near the curves represent the appropriate values of F_0 in MW cm^{-2}. Curve 1 in figure 4(a) is the low-intensity laser pulse whose shape is undistorted due to the interaction with the suspension. As can be seen in figure 4(a), with an increase in F_0 the transmitted laser pulse becomes shorter and the pulse peak shifts towards

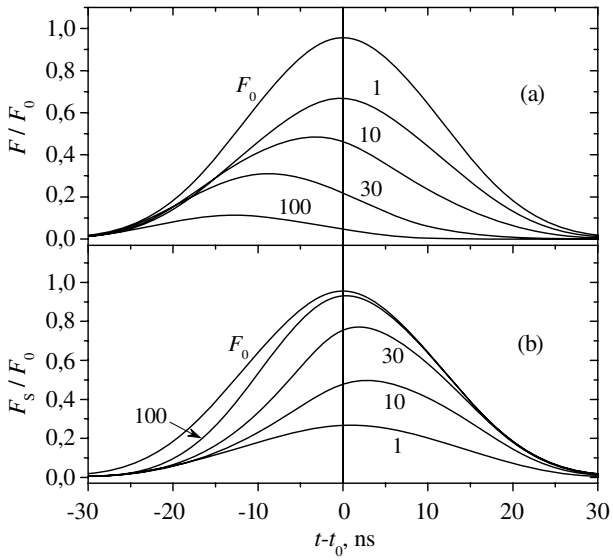

Figure 3. The calculated oscillograms of transmitted (a) and scattered (b) laser pulses. Numbers near the curves are the values of F_0 in MW cm^{-2}. Curves marked as F_0 are the oscillograms of the incident laser pulse.

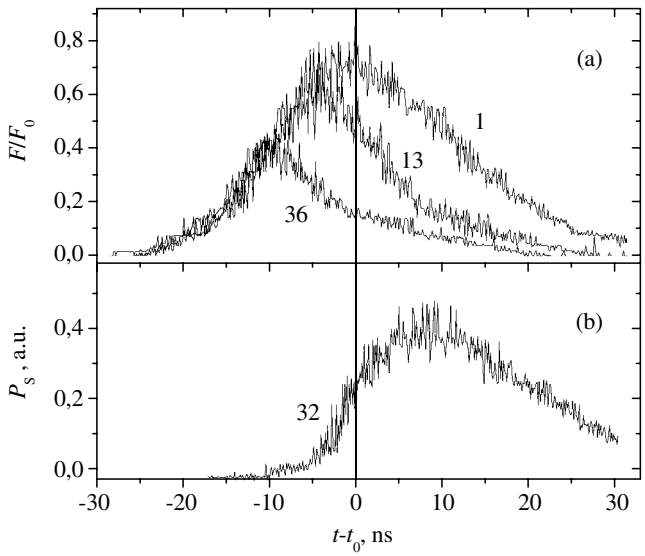

Figure 4. The experimental oscillograms of transmitted (a) and scattered (b) laser pulses. Numbers near the curves are the values of F_0 in MW cm^{-2}.

the pulse front. The pulse width, τ_i, and the pulse peak shift, Δt_m, are plotted in figure 5 as a function of incident laser power F_0. In this figure the solid curves are calculated similarly to those in figure 3. The agreement between the experimental and calculated values in figure 5 is satisfactory.

The model under consideration assumes that the self-induced attenuation of laser radiation results from the growth of gaseous shells around the laser-heated suspended particles. The

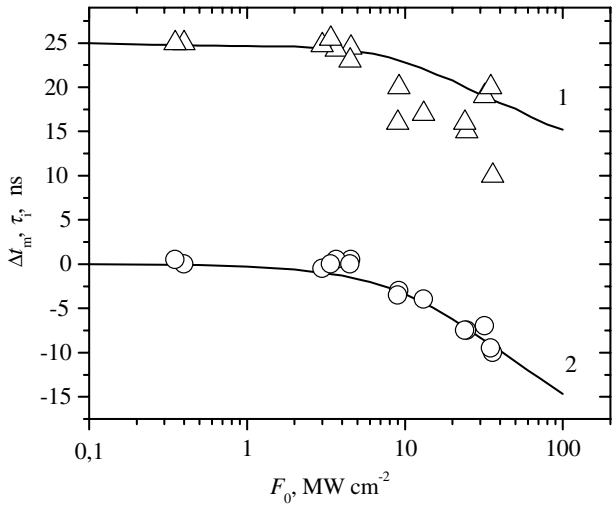

Figure 5. The transmitted pulse width (1) and the pulse peak shift (2) as functions of F_0. Open symbols: experiment; solid curves: calculation.

calculations show that the extinction cross-section $\sigma(t)$ increases by a factor of 5–10 during the laser pulse. So we can expect that the pulse shape of the scattered laser radiation will differ from the shape of incident and transmitted laser pulses because scattering is much stronger at the end of the laser pulse. The integral power, P_S, of laser light scattered within the solid angle $\Delta\Omega$ can be written as

$$P_S(t) = \int_0^d \frac{d\sigma(z,t)}{d\Omega} \Delta\Omega F(z,t) N S_0 \, dz \tag{6}$$

where S_0 is the laser beam cross-sectional area. The appropriate calculated oscillograms are given in figure 3(b), where $F_S = P_S/S_0$. As can be seen from the figure, the shapes of incident, transmitted and scattered pulses are very different. The scattered pulse is delayed for several nanoseconds compared with the incident pulse and this delay is a function of F_0. The experimental evidence of a scattered pulse delay is given in figure 4(b) which presents an oscillogram recorded at a scattering angle of approximately 20° at $F_0 = 32$ MW cm^{-2}. The experiments show that the measured delays of scattered pulses are approximately twice as large as the calculated values (see figure 3(b)).

For the phenomenon investigated in this work and caused by the scattering of laser light, the problem concerns the separation of the transmitted and forward-scattered light. The following additional measurements of optical transmittance were taken with the use of a variable-diameter diaphragm installed in front of the photodetector registering the transmitted laser light. As can be seen from figure 6, curve 1, at low laser power the transmittance T_0 is practically independent of the diaphragm diameter D, and hence we conclude that light scattering plays a minor role in T_0. At larger F_0, the transmittance slightly increases with D (see figure 6, curves 2 and 3), thus indicating the presence of scattered laser light in the transmitted optical signal. Note that the experimental transmittance data presented in figure 1 were obtained with the photodetector angular aperture set at approximately 0.05, which corresponds to $D = 6$ mm in figure 6. This circumstance may be one of the reasons for the difference between the measured and calculated transmittance at $F_0 > 30$ MW cm^{-2} in figure 1.

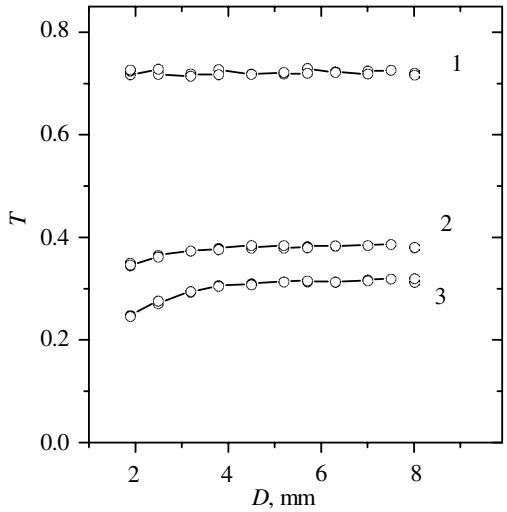

Figure 6. The cell transmittance, T, as a function of diaphragm diameter, D. $F_0 = 1$ MW cm^{-2} (curve 1), 18 MW cm^{-2} (curve 2), 30 MW cm^{-2} (curve 3).

Commenting further on the data presented in figure 2, for a particular low excitation level, the calculations of γ were performed in [9] with the use of the heat balance equation

$$\sigma_0 F_0 = \text{constant} \times \theta_p S \tag{7}$$

where S is the area through which the particle loses its energy by thermal conduction, and θ_p is the average temperature of a laser-heated particle. This implies that

(i) the laser excitation is reasonably low in order for other mechanisms of particle energy loss (thermal emission, evaporation of the particle's material, plasma formation, etc) to be neglected, and
(ii) the excitation is sufficiently high so that the particle temperature is well above ambient temperature.

For the calculation of γ, the particle temperature from (7) should be substituted into Plancks formula for black-body emission. According to the calculations [9], at a wavelength of 500 nm, the values of $\gamma = 3$–7 correspond to a particle temperature of 16 000–5000 K. The range of $\gamma < 3$ at $\lambda = 500$ nm was not considered in [9] because of the uncertain huge values of estimated particle temperature (up to 10^5 K). Also, the approach considered in [9] is completely irrelevant for the case of $\gamma \leqslant 1$. Thus, to give a qualitative assessment of the experimental data presented in figure 2, the following reasons are considered. According to the estimate of the parameter G obtained, we leave unaltered the assumption [8, 9] that the primary mechanism of particle energy dissipation is heat transfer to the environment. In other words, equation (7) is used. (Here we also neglect the particle energy loss due to the generation of acoustic pulses [23].) As for the dimensions of core–shell particles that increase with an increase of F_0, it is plausible that the area S in (7) is not a constant but also increases with F_0, for example, as consequence of (2). Then, according to (7), the dependence of particle temperature on F_0 becomes sublinear and causes an additional decrease in the values of γ.

Finally, it should be noted that the proposed model describes the interaction of laser radiation with a suspension of light-absorbing particles only during the action of the laser pulse. Because the model does not consider relaxation processes, it cannot predict the behaviour of

laser-heated particles after the end of the laser pulse. Here we simply note that the preliminary experiments reveal a relatively long time of relaxation (in the range of milliseconds) of laser-induced attenuation in the suspension.

4. Concluding remarks

In this work the interaction of powerful laser radiation with an aqueous suspension of submicron light-absorbing particles was investigated in the range of laser intensities of tens of megawatts per square centimetre. The results obtained indicate that the processes of water evaporation around the laser-heated particles play a significant role both in the attenuation of laser radiation propagating through the suspension and in the formation of LII optical signals. The proposed model of the interaction of suspended particles with laser radiation describes the experimental data with satisfactory agreement. The model considers only one aspect of the problem—the evaporation of the surrounding water. With respect to the particle energy balance, this mechanism is not a primary one. However, it is the one which primarily determines the attenuation and scattering of powerful laser radiation in the suspension.

References

[1] Vander Wal R L 1996 *Appl. Opt.* **35** 6548–59
[2] Vander Wal R L and Weiland K J 1994 *Appl. Phys.* B **59** 445–52
[3] Vander Wal R L 1996 *Combust. Sci. Technol.* **118** 343–60
[4] Witze P O, Hochgreb S, Kayes D, Michelsen H A and Shaddix C R 2001 *Appl. Opt.* **40** 2443–52
[5] Cignoli F, Benecchi S and Zizak G 1994 *Appl. Opt.* **33** 5778–82
[6] Allouis C, Rosano F, Beretta F and DAlessio A 2002 *Meas. Sci. Technol.* **13** 401–10
[7] Eckbreth A C 1977 *J. Appl. Phys.* **48** 4473–9
[8] Zelensky S 1998 *J. Phys.: Condens. Matter* **10** 7267–72
[9] Zelensky S 1999 *J. Opt. A: Pure Appl. Opt.* **1** 454–8
[10] Zelensky S 2003 *J. Lumin.* **104** 27–33
[11] Kafalas P and Ferdinand A P 1973 *Appl. Opt.* **12** 29–33
[12] Wood C F, Leach D H, Zhang J Z, Chang R K and Barber P W 1988 *Appl. Opt.* **27** 2279–86
[13] Pinnick R G, Biswas A, Armstrong R L, Jennings S G, Pendleton J D and Fernandez G 1990 *Appl. Opt.* **29** 918–25
[14] Alexander D R and Armstrong J G 1987 *Appl. Opt.* **26** 533–8
[15] Park B S and Armstrong R L 1989 *Appl. Opt.* **28** 3671–80
[16] Prishivalko A P 1983 *Sov. Izv. Phys.* **26** 46–52
[17] Pendleton J D 1985 *Appl. Opt.* **24** 1631–7
[18] Xie J G, Ruekgauer T E, Armstrong R L and Pinnick R G 1991 *Phys. Rev. Lett.* **66** 2988–91
[19] Kwok H S, Rossi T M, Lau W S and Shaw D T 1988 *Opt. Lett.* **13** 192–4
[20] Venger E F, Goncharenko A V and Dmitruk M L 1999 *Optics of Small Particles and Disperse Media* (Kiev: Naukova Dumka)
Shifrin K S 1951 *Light Scattering in Turbid Media* (Moscow: GITTL)
[21] Kim D, Park H K and Grigoropoulos C P 2001 *Int. J. Heat Mass Transfer* **44** 3843–53
[22] Kim D, Ye M and Grigoropoulos C P 1998 *Appl. Phys.* A **67** 169–81
[23] Park H K, Kim D, Grigoropoulos C P and Tam A C 1996 *J. Appl. Phys.* **80** 4072–81